Journal of Magnetic Resonance 199 (2009) 75–87

Contents lists available at ScienceDirect

Journal of Magnetic Resonance

journal homepage: www.elsevier.com/locate/jmr

Chemical-shift referencing and resolution stability in gradient LC–NMR (acetonitrile:water)

Paul A. Keifer *

Varian Inc., 3120 Hansen Way D-298, Palo Alto, CA 94304-1030, USA

ARTICLE INFO

Article history:
Received 23 December 2008
Revised 14 March 2009
Available online 21 April 2009

Keywords:
LC–NMR
Referencing
Reference standards
Lineshape
Magnetic susceptibility

ABSTRACT

Wide ranges of solvent conditions are generated during solvent-gradient LC–NMR. This complicates the referencing of the chemical-shift scale of the resulting NMR data. The problems that arise when performing LC–NMR in acetonitrile:water – particularly when the mobile-phase composition can range anywhere from 0% to 100% – are examined here, and the reliability of the secondary reference signals are evaluated. It is shown that under these conditions the use of the acetonitrile signal is superior to the use of the water signal in any form (either the ^{1}H or the ^{2}H signal) as a secondary reference, a lock signal, and a signal for shimming. The limitations of the referencing methods and other experimental parameters, and the limitations on the solvent-gradient ramp parameters, primarily as they affect lineshapes, are all shown. These results are compared to the way some other publications have referenced the ^{1}H chemical-shift axis (when using acetonitrile:water mixtures to perform reversed-phase chromatography LC–NMR).

1. Introduction

An important part of NMR spectroscopy is the referencing of the chemical-shift scale so that proper peak positions can be determined [1]. In solution-state ^{1}H NMR (in $CDCL_3$ samples), this is sometimes accomplished by adding the primary reference standard TMS (tetramethylsilane) directly to the sample [2]. Alternatively, a secondary reference standard such as the ^{1}H resonance of $CDCl_3$ (or other solvent signal) can be used, once its chemical shift (relative to TMS) has been determined.

In addition to the choice of whether to use either a primary or a secondary reference standard (i.e., which compound is used to generate the signal), there are three general methods to accomplish the referencing [1]. The first is to use an internal standard [2]. The second is to use a lock signal (typically the ^{2}H signal of the solvent). The third is to use an external sample. This "external sample" method may use either the "substitution method" (the traditional method of swapping NMR tubes and running another spectrum; in which the sample and the reference are in different NMR tubes), or by having two tubes in the magnet simultaneously (one with the reference and another with the sample; using coaxial tubes or not; using either an internal lock or an external lock), or by adjusting the lock frequency on the spectrum of one unlocked sample so as to make the spectrum of the next (unlocked) sample properly referenced [3].

The use of these three general methods to reference NMR spectra is well documented for conventional solution-state NMR spectroscopy, but the referencing process is less consistent for flow NMR techniques [4] that use solvent gradients, such as LC–NMR or LC–NMR–MS. (Henceforth in this paper, the term "LC–NMR∗" will be used to generally refer to all the various different hyphenation and hypernation [5] permutations of the technique, such as LC–NMR, LC–NMR–MS, and LC–UV–NMR–MS, etc.) LC–NMR∗ has some additional chemical-shift-referencing issues that have not been fully addressed by IUPAC conventions [1]. It appears to be unique in the NMR world in terms of the kinds and number of sources of variability (errors) in the referencing process. This paper documents these variables for a mobile phase composed of acetonitrile:water (either CH_3CN:D_2O or CH_3CN:H_2O), because this is the most commonly used mobile phase in LC–NMR∗. It shows the effects of solvent gradients (as used for chromatographic elution) running from 0% to 100% (by volume) CH_3CN, so as to cover the entire range of solvent-gradient and solvent-composition behaviors. This paper focuses on the referencing errors that arise from using the first and second referencing methods discussed above – the "internal standard" and the "lock signal" methods – and it will focus exclusively on ^{1}H-observe spectra.

IUPAC has proposed that the primary reference standard for ^{1}H spectra be "1% by volume TMS in $CDCl_3$" set to 0.0 ppm (with the chemical-shift scales of all X nuclei determined from here) [1,6]. In reversed-phase LC–NMR∗, TMS is not a useful option, both because of its limited solubility in the polar aqueous mobile phases used and because it can be retained on LC columns. For working in water, DSS (sodium 2,2-dimethyl-2-silapentane-5-sulfonate)

* Fax: +1 650 852 9688.
E-mail address: PAKeifer@gmail.com

1090-7807/$ - see front matter © 2009 Elsevier Inc. All rights reserved.
doi:10.1016/j.jmr.2009.04.010

[7–9] and TSP (sodium 3-(trimethylsilyl) propanoate) [9,10] have been proposed as alternative internal reference compounds (and DSS is considered in practice to have the same chemical shift as TMS) [1]. (Note that the literature sometimes reverses the abbreviations DSS and TSP [11].)

When solvent gradients are used in LC–NMR∗, the composition of the mobile phase changes during the NMR acquisition. (In this respect, LC–NMR∗ may be unique among NMR applications.) As the solvent-composition changes, the NMR resonances move. Chemical-shift reference standards are well known to undergo changes in their chemical shifts when dissolved to differing concentrations in solutions (caused by mixing samples with different bulk magnetic susceptibilities and by other solvent-association effects) [12–14]. The ^{1}H chemical shift of the TMS resonance has been found to be dependant upon solvent, pH, concentration, temperature, and sample shape and orientation [15–19], and it moves as much as 0.23 ppm (for 1% TMS solutions) [20] or more [12] when it is dissolved in different solvents. The ^{1}H chemical shift of DSS moves upfield by ~0.1 ppm as a function of concentration (ranging from 0.5% to 5% by weight; 0.023–0.23 M) [3]. The ^{1}H chemical shifts of DSS and TSP are sensitive to pH and ionic strength [8,21–23], and they also move upon interaction with other molecules (i.e., purine and proteins, and cyclodextrins), which caused some studies to use other internal reference standards [9,24–26]. (It was also shown, by LC–NMR, that the ^{29}Si chemical-shift-reference standards hexamethyldisilane (HMDSS) and octamethyltrisiloxane (OMTSO) undergo large chemical-shift movements during solvent gradients [27].) So it is well documented that the ^{1}H chemical shifts of conventional solution-state reference standards can move as a function of solvent, temperature, concentration, pH, ionic strength, and the presence of other compounds.

Other secondary chemical-shift reference compounds have been used for specific ^{1}H NMR applications. Formate has been used for acquiring ^{1}H spectra of serum, because it does not interact with protein macromolecules in the serum (unlike TSP) [28]. Hexamethyldisiloxane has been used in organic solvents to improve quantitation [14]. Both DSA (4,4-dimethyl-4-silapentane-1-ammonium trifluoroacetate) and dioxane have been used for protein samples because they were shown to not interact with proteins [25,29]. The internal standard *N*,*N*′,*N*″-trimethyl(2-trimethyl) ethylammonium iodide (TMS-A) was proposed as a way to minimize some of the limitations of TSP and DSS [30], and other compounds have been proposed to minimize some of the limitations of TMS [31–33].

The ^{1}H signal of H_2O (or HOD) was sometimes used as a *primary* chemical-shift reference standard decades ago [34,35], but that stopped long ago when it was observed how much the water resonance moved as a function of temperature, pH, ionic strength, and concentration [8,36] (which presumably occurs largely due to changes in hydrogen bonding). Currently, water sometimes serves as a *secondary* chemical-shift standard, typically for ^{1}H NMR of biochemical samples [22], but only because its chemical shift as a function of temperature has been well documented [8,23,36]. It is less well documented how much the chemical shift of water in a mixture depends upon the composition of the mixture (mostly because it can be quite variable), although this effect was observed in the very early days of NMR [37]. In 1958, Schneider et al. showed that the chemical shift of water changes as much as 4.58 ppm between a solution-phase and a gas-phase sample [38]. In our data (which is solution-phase LC–NMR∗ only), we can easily see the water resonance move over a 2.4 ppm range, as is shown in Fig. 1. The proton chemical shift of water is also well known to have a large dependence upon sample temperature [39,40], and a dependence upon the concentration of dissolved solute [26].

In modern solution-state NMR, TMS always serves as only a primary-reference internal standard (although the ^{1}H signal of TMS was also used as a lock signal decades ago [14]). In contrast, a solvent signal like $CDCl_3$ can serve as either an internal standard (by referencing to its residual ^{1}H resonance) or as a lock reference (by locking on the ^{2}H signal). LC–NMR∗ experiments present more complicated choices. First, when CH_3CN:D_2O or CH_3CN:H_2O mixtures are used as the mobile phase, one could use either the water or the acetonitrile signals for ^{1}H-chemical-shift referencing. Second, the water could serve as either an internal standard (when using the ^{1}H resonance of H_2O or HOD) or as a lock signal (when using the ^{2}H resonance of D_2O or HOD). (In LC–NMR∗, D_2O is often used in place of H_2O because it is a relatively inexpensive way to

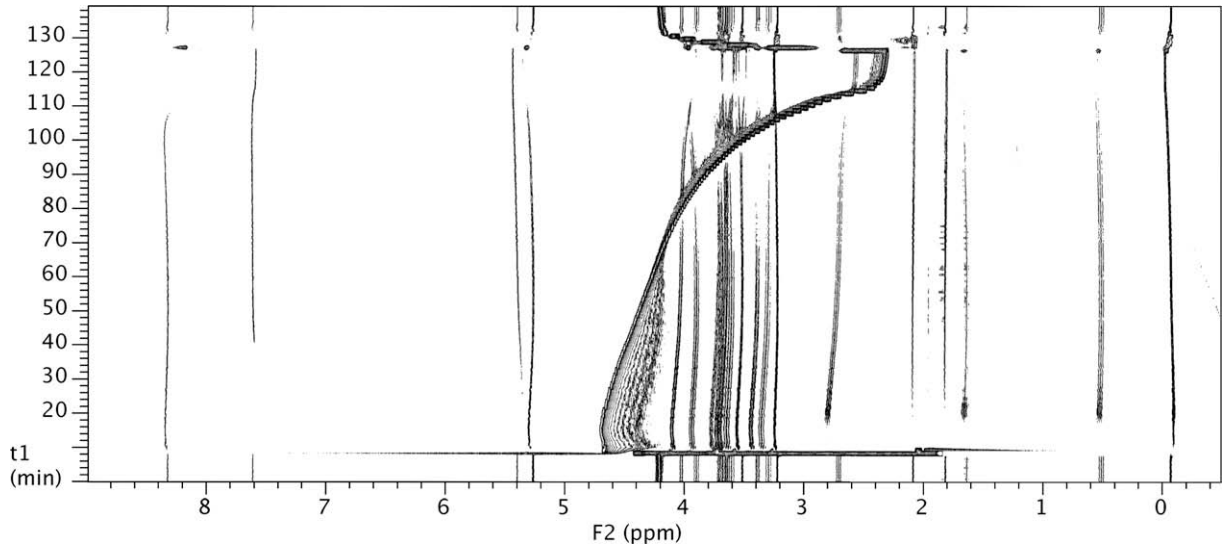

Fig. 1. Single-frequency suppression. This is LC-NMR data acquired with single-frequency solvent-suppression (on CH_3CN only, no HOD suppression) so as to more easily see the movement of the HOD resonance during the solvent gradient. In this experiment, the transmitter was actively maintained on the CH_3CN resonance. The resulting 2.4-ppm movement of the water resonance tracks the solvent composition shown graphically in Fig. 2. Due to the void volume of the plumbing and the signal-averaged nature of the NMR acquisitions, there is a ca. 3-min lag time (ca. 3 mL at the flow rate of 1 mL/min) between when the solvent-composition changes at the HPLC pumphead and the ^{1}H resonances in the NMR flow cell reflect the change. (Acquired with 16 transients per increment, a 1% ramp at 1 mL/min, and no ^{2}H lock.)

reduce solvent background signals and it provides a ^{2}H lock.) In contrast, the CH_3CN can serve only as an internal standard. (Although the Scout-Scan method used here and described below does allow the CH_3CN signal to essentially function as a field/frequency lock.)

The data presented here show that many problems can occur when using the water signal for *any* purpose – either as a ^{1}H reference, or as a ^{2}H lock, or for shimming. It shows how the ^{2}H lock on D_2O or HOD actually creates chemical-shift instability. It also shows that the acetonitrile signal is superior to the water signal for all of these purposes. (Note that, if deuterated acetonitrile (CD_3CN) is used and you use a ^{2}H lock on the CD_3CN, the chemical-shift scale will be well-behaved, however this case will not be discussed here further.)

2. Results

2.1. The HPLC method

During LC–NMR* experiments that use solvent gradients, the HPLC method controls the solvent composition as a function of time. Whenever the HPLC method makes a change in the solvent composition (which happens immediately at the HPLC pumphead), that change will propagate through the HPLC column and assorted tubing to the NMR probe. When the solvent-composition changes within the NMR probe, this causes the frequencies of all the ^{1}H resonances to move – including the solvent resonances.

The mobile phase used in this study was a binary mixture of CH_3CN and D_2O, each spiked with a cocktail of additives (whose resonances serve as chemical-shift change monitors; as described below). The HPLC method used here is diagrammed in Fig. 2. This figure is generic in that the duration of the gradient ramp, in both time and solvent volume, was changed in different runs. Although some of the solvent-composition changes are sudden, the change of primary interest is the slow ramp from 0% to 100% CH_3CN in the middle of the HPLC method.

2.2. Solvent suppression and referencing

The solvent resonances were typically large enough that we suppressed both the CH_3CN and the HOD resonances. (D_2O typically absorbs enough H_2O to form an observable amount of HOD during LC–NMR* unless significant precautions are taken.) One way to accomplish the suppression is to use a two-frequency shaped (WET [41]) pulse in which the transmitter is kept on one resonance and the other resonance is irradiated by the SLP (shifted laminar pulse; phase-ramped pulse) technique [42]. This requires the user to decide which of these two resonances to keep the transmitter on – either the CH_3CN or the HOD. These two cases are not equivalent, and the choice has a big impact upon the resulting data, as is shown below.

Whenever the solvent resonances move (due to solvent-composition changes) the frequencies used for solvent suppression need to be re-optimized. The rate at which this needs to happen depends upon the rate of change of solvent composition, which is influenced by the flow rate and the HPLC method (which are both under user control). It is also influenced by how much each resonance moves in response to changes in solvent composition (which is not under user control). We are using the Scout-Scan technique [41,43] to automatically re-optimize these frequencies for every increment (spectrum) of the pseudo-2D data. The Scout-Scan technique first takes a small-tip-angle ^{1}H spectrum without using solvent suppression, analyzes that spectrum to both set the transmitter on the desired resonance and calculate the resulting frequency offset(s) for the solvent signal(s) to be suppressed, creates a shaped pulse that excites all these resonances (using Pbox [44,45] and the 90°-pulse calibration information), then it resets the parameters to do a signal-averaged solvent-suppressed ^{1}H spectrum and starts acquisition. The entire Scout-Scan process takes just a few seconds. The frequency at which this happens is determined by the number of transients used per spectrum (our default was 16). Also under user control are the number of resonances searched for, whether to use ^{13}C-satellite suppression, and which resonance to keep at a constant chemical shift. All data shown here were acquired using WET solvent suppression and the Scout-Scan technique.

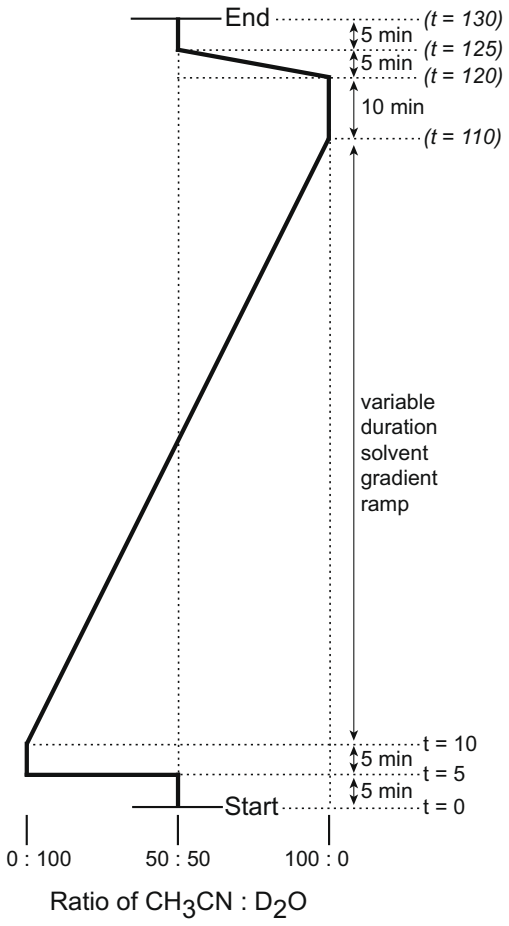

Fig. 2. A generic diagram of the HPLC method used in these studies. The diagram is oriented with time along the vertical axis ($t = 0$ at the bottom) and the solvent composition along the horizontal axis, so as to best facilitate visual comparisons with the LC-NMR data in the other figures. The fixed times within the HPLC method are indicated along the right-hand edge. The duration of the solvent-gradient ramp was a variable in different experiments, so absolute times after the ramp were not fixed. The absolute times shown in italics within parentheses correspond to those used for the default solvent-gradient ramp (which had a 1% solvent-composition change per minute ramp over a 100-min period). Both the CH_3CN and the D_2O (HOD) contained multiple additives that served as chemical-shift markers, as is described in the text.

To get good data you need to reference the multiple spectra (increments) within the pseudo-2D dataset. The normal way to do this is to actively maintain one resonance at a constant chemical shift. The Scout-Scan technique does this by actively adjusting the transmitter (the center of the spectrum) for every spectrum onto one of the tall resonances, which in this solvent system would be either the CH_3CN or the HOD resonance.

Fig. 1 shows the movement of the HOD and CH_3CN resonances relative to each other. This dataset was acquired by actively maintaining the transmitter on the CH_3CN resonance, and referencing the CH_3CN resonance in every increment of the pseudo-2D experi-

ment to 1.95 ppm. Only single-frequency (CH_3CN) solvent suppression was used here to allow the water resonance to be seen more easily. (The HOD signal is much smaller than the CH_3CN signal due to the predominance of D_2O over H_2O.) This figure shows that the water resonance moves 2.38 ppm relative to the CH_3CN resonance during the 0–100% CH_3CN ramp. (We show below that the frequency of the CH_3CN resonance actually remains rather constant, and serves as an appropriate secondary reference compound.)

To more carefully evaluate the relative movement of the ^1H resonances from different compounds, we spiked the mobile phase with a variety of compounds whose relative ^1H chemical-shift movements could be monitored during the 0–100% solvent-gradient ramp. The selection of the mobile-phase additives was challenging because they had to be soluble in both solvents (CH_3CN and D_2O), not unduly retained by the chromatographic column, and we also wanted sharp ^1H resonances so we could measure lineshape distortions. We finally settled on a cocktail that contained DSS (sodium 2,2-dimethyl-2-silapentane-5-sulfonate), CH_3CN, CH_3OH, sucrose, H_2O, CH_2Cl_2, $CHCl_3$, and sodium formate. Their chemical shifts in 50:50 CH_3CN:D_2O (the starting conditions) as shown in Fig. 3 were (with CH_3CN set to 1.95 ppm): DSS = −0.079 ppm (singlet) and multiplets at 0.5, 1.6, and 2.7 ppm; CH_3CN = 1.95 ppm (singlet; used as the secondary reference signal); CH_3OH = 3.31 ppm (CH_3 group, singlet); sucrose = multiplets ranging from 3.3 to 4.2 ppm, and a doublet at 5.25 ppm (J = 3.9 Hz); HOD = 4.2 ppm; CH_2Cl_2 = 5.4 ppm (singlet); $CHCl_3$ = 7.6 ppm (singlet); and formate = 8.3 ppm (singlet).

Some of these additives were partly retained on the chromatography column under 100% D_2O conditions, which influenced the design of the HPLC method. To better visualize every resonance from each additive, the HPLC method was started at 50:50 CH_3CN:D_2O (to equilibrate the system) then changed to 100% D_2O for 5 min (between t = 5 and t = 10 min) before starting the solvent-gradient ramp at t = 10 min (Fig. 2). This allowed reproducible amounts of additives to be retained on the HPLC column for each run, and also allowed each LC–NMR dataset to have multiple "control" spectra at the beginning of each run where all of the ^1H resonances were visible (for lineshape verification). The sudden solvent change from 50:50 to 0:100 CH_3CN:D_2O usually generated several increments worth of "ugly" spectra, but this was considered to be an acceptable tradeoff to ensure a reproducible method. (The spectra became "ugly" because such a sudden radical solvent change moves all the resonances during one single increment while the NMR spectrometer continues to signal average. Also, the lineshape of every resonance became grossly deteriorated due to magnetic-susceptibility inhomogeneities in the NMR flow cell caused by incomplete mixing of the incoming solvent. Both effects show why there are limitations in how rapidly the solvent composition can be changed during an LC–NMR* experiment. Typically, the solvent composition should only be changed by 1–2% per minute or else the spectral data quality will suffer, as shown below.) Finally, after the solvent-gradient ramp reached 100% CH_3CN, the HPLC method returned to a 50:50 solvent composition (more gently this time) to have additional "control" spectra at the end of each run.

When acquiring LC–NMR* data, probably the most fundamental and important choice a user needs to make is whether to maintain the transmitter on the CH_3CN or the HOD resonance. We designed the additive cocktail and the HPLC method to help us evaluate this choice. Figs. 4 and 5 illustrate the ramifications of this choice. Fig. 4 was acquired by actively maintaining the transmitter on the CH_3CN resonance for each increment (and referencing the CH_3CN resonance to 1.95 ppm). Fig. 5 was acquired by actively maintaining the transmitter on the HOD resonance (and referencing the

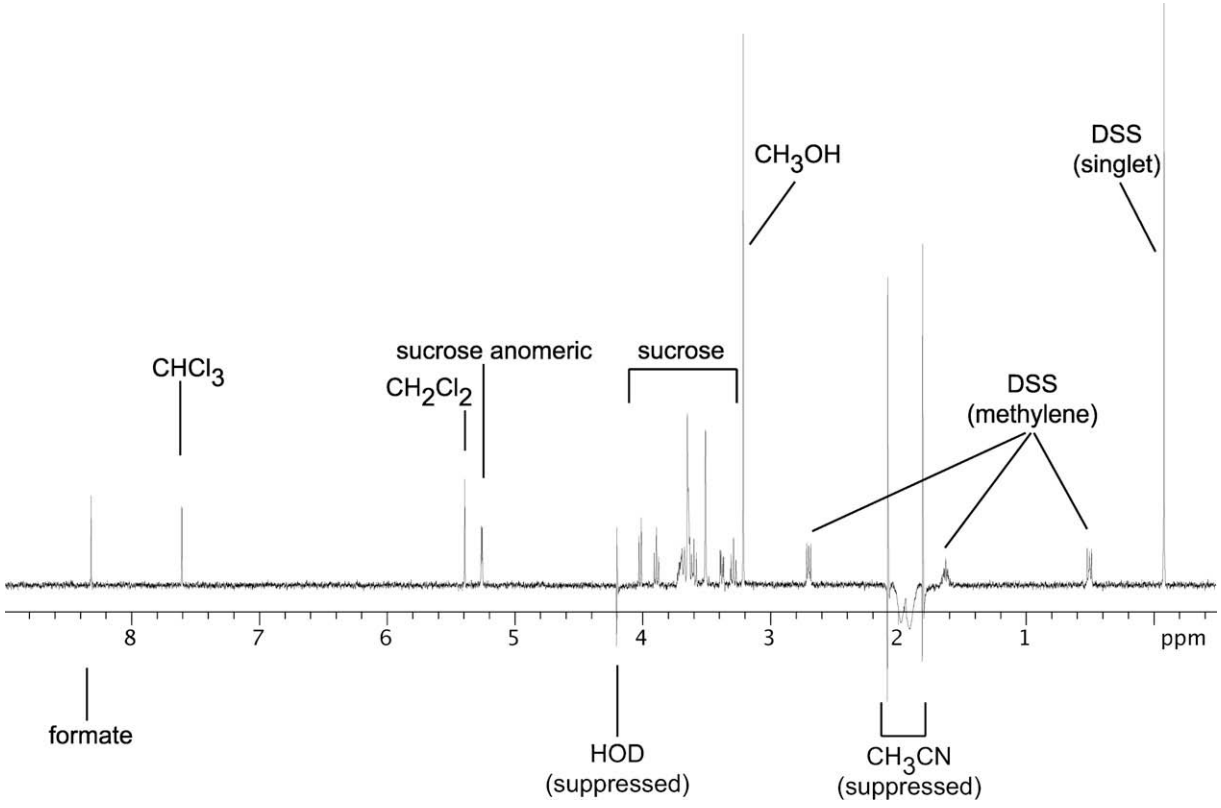

Fig. 3. A ^1H spectrum of the mobile phase and its additives. This spectrum was acquired at an equilibrated solvent composition of 50:50 CH_3CN:D_2O using two-frequency WET suppression. The resonances of the additives are labeled. The CH_3CN was used as a secondary reference signal and assigned a value of 1.95 ppm, which places the DSS singlet at −0.079 ppm in this solvent composition. (This spectrum was acquired with 32 scans and a ^2H lock, and was processed with 0.4 Hz linebroadening, threefold zerofilling, and solvent subtraction on the residual CH_3CN signal [ssfilter = 60].)

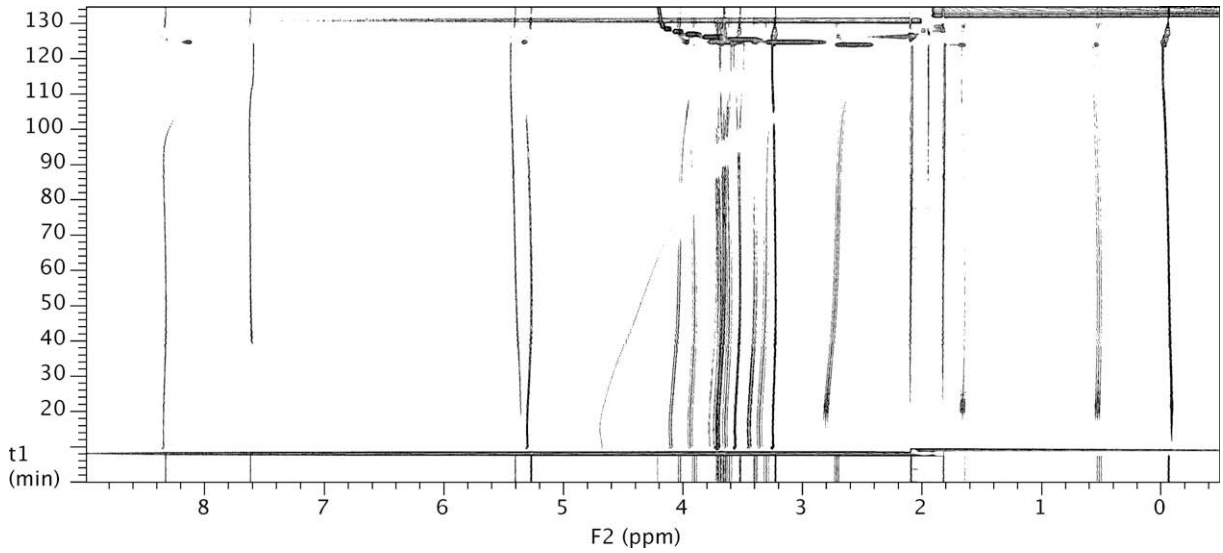

Fig. 4. Two-frequency suppression; CH_3CN centric. This LC-NMR data was acquired identically to that shown in Fig. 1 (transmitter maintained on CH_3CN) except that now two-frequency solvent suppression was used. Although the chemical-shift changes undergone by the water are now harder to see than in Fig. 1, it is easier to monitor the chemical-shift changes in the resonances of all the other compounds. (Acquired without using a ^2H lock.)

HOD resonance to 4.19 ppm). (Referencing the HOD signal to 4.19 ppm was used here because this placed the CH_3CN resonance in 50:50 CH_3CN:D_2O at 1.95 ppm, which facilitated comparisons between datasets within this study.)

The first observation extracted from these figures is that the chemical shifts arising from all the additives are generally constant when CH_3CN is kept on resonance (Fig. 4). The HOD signal is the only signal that moves a lot (2.38 ppm, as was shown more clearly in Fig. 1). In contrast, when the HOD signal is kept on resonance (Fig. 5), the resonances of all the additives move extensively. This demonstrates that holding the HOD resonance constant is artificial and it causes unacceptable distortions in chemical shifts.

2.3. The ^2H lock

Although the water-centric Fig. 5 was acquired by actively maintaining the transmitter on the HOD resonance (using the Scout-Scan method), the same result is obtained if the ^2H lock is used alone (without any form of Scout-Scan-type correction; data not shown). This is because the only available ^2H signal in the solvent system used here (the commonly used CH_3CN:D_2O) is D_2O (or HOD). The ^2H lock holds the ^2H resonance of D_2O/HOD at a fixed frequency, which then holds the ^1H resonance of HOD/H_2O at a fixed frequency (because they track together), unless an additional correction mechanism is used. This is why the use of the ^2H lock alone (without a Scout-Scan resetting of the transmitter frequency) also produces unacceptable spectra.

The ^2H-lock problem is actually worse than that. The previous paragraph explains why the use of only the ^2H lock on D_2O/HOD mis-sets the chemical-shift scale within the entire LC–NMR* dataset by up to 2.38 ppm. We can also see that the ^2H lock causes a related problem *within* each increment. The tugging of the ^2H lock (on D_2O/HOD) that happens *during* a signal-averaged increment manifests itself as a broadening of all the other resonances within

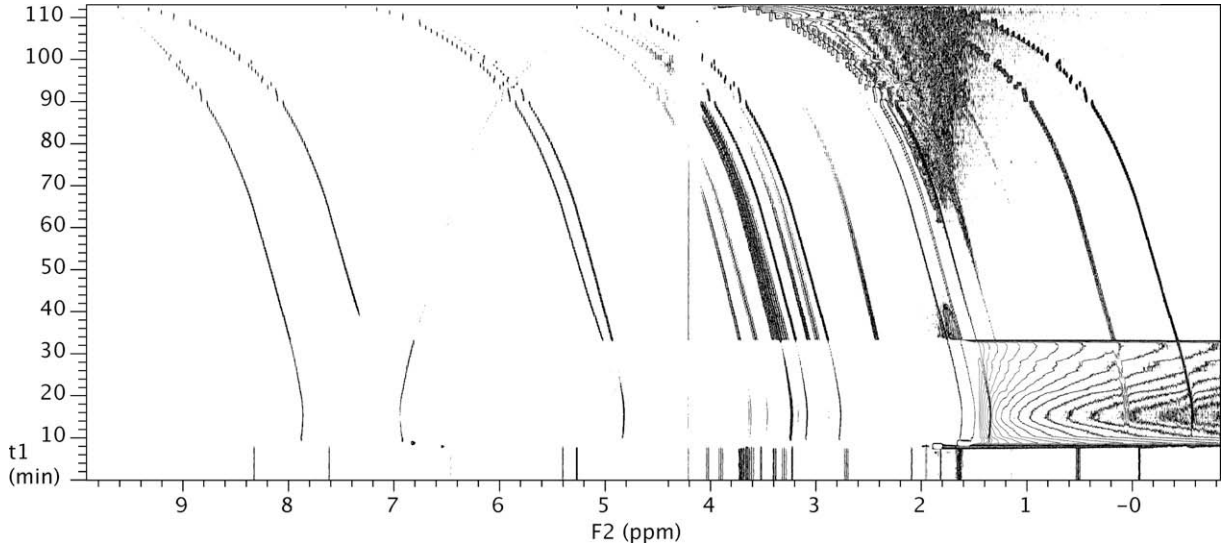

Fig. 5. Two-frequency suppression; HOD centric. This LC-NMR data was acquired identically to that shown in Fig. 4 except that now the transmitter was maintained on the HOD resonance instead of the CH_3CN resonance. The very-low intensity signals that curve from the lower left to the upper right (stating at 6.9 ppm) are low-intensity quadrature images arising from the large off-resonance CH_3CN resonance, which are present only because an analog receiver was used and are not present on direct-digital receiver data. (Acquired without using a ^2H lock.)

each spectrum (increment). Fig. 6 shows this effect on an expansion of the DSS singlet, which is a narrow resonance unless it is broadened by a wandering D_2O resonance that tugs on the ^2H lock. Figs. 6 and 1 together show that when the ^1H HOD resonance moves most rapidly in Fig. 1 (increasingly from 90 to 115 min), the DSS resonance in the "Locked" spectrum (on the right-hand side of Fig. 6) suffers the most linebroadening (as compared to the "Unlocked" spectrum on the left-hand side of Fig. 6).

2.4. The solvent-gradient ramp

Whenever the solvent-gradient ramp becomes steeper in time or volume, the solvent mixture in the NMR flow cell become more inhomogeneous (in magnetic susceptibility), which in turn broadens the NMR resonances. This heterogeneity is due either to incomplete mixing of the contents of the flow cell, or to ramps that are too steep for the volume of the NMR flow-cell used. (Smaller NMR flow cells tolerate steeper solvent ramps, but also decrease the inherent NMR sensitivity.) During steep solvent-gradient ramps, the potential for inappropriate chemical-shift tugging by the ^2H lock becomes greater, because the lock is tracking a D_2O/HOD resonance that moves and broadens faster as the solvent-composition ramps faster. This effect is shown in Fig. 7, which compares datasets acquired with 0–100% CH_3CN ramps (all flowing at 1 mL/min) that occurred over 100 min (1%/min), 50 min (2%/min), 25 min (4%/min), and 12.5 min (8%/min). Although the left-hand spectrum still has a narrow DSS linewidth throughout the experiment, the DSS linewidth gets broader and less uniform as the solvent-gradient ramp becomes ever faster (the three right-most spectra). Note that this linebroadening is caused by the steepness of the solvent gradient, and cannot be removed by shimming.

The linebroadening caused by the steepness of the solvent-concentration ramp is influenced by both the volume- and time-steepness of the ramp. Fig. 8 shows that if the ramp is kept steep in volume, but made slow in time, then the effect of poor mixing within the NMR flow cell can be reduced. The left-most spectrum was acquired with a 0–100% ramp of 8%/mL over a period of 12.5 min at a flow rate of 1.0 mL/min (8%/min). The middle spectrum was acquired with a 0–100% ramp of 8%/mL, but now pumping 20-fold slower over a 20-fold longer time (the flow rate was 0.05 mL/min over 250 min, giving a ramp rate of 0.4%/min). The right-most spectrum is a control spectrum that shows the DSS lineshape during a 1%/mL ramp over 100 min, at 1.0 mL/min, so 1%/min. These three spectra show that if the flow rate is slow enough, it may compensate for a solvent-gradient ramp that is steep in volume.

Similar but less dramatic effects can be seen with shallower solvent ramps. A comparison of data acquired with 0–100% ramps over either 100 min at 1.0 mL/min (1%/min) or 800 min at 0.5 mL/min (0.125%/min) shows that the DSS linewidth remains narrower for the slower, shallower-ramp run (data not shown) as is expected. (The signal-to-noise is also higher for the slower-ramp dataset because the slower pumping speed allows more scans per increment to be used with no penalty. This is a general principle in LC–NMR*.)

2.5. Diffusion

The good DSS lineshape in the middle spectrum of Fig. 8 could be due to either more time for active diffusion within the NMR flow cell (which would actively render the magnetic susceptibility homogeneous over time) or to the lack of "jetting" of fresh solvent into the flow cell (which avoids creating the inhomogeneity in the first place). To evaluate this, the "8%/min 8%/mL" experiment was repeated, but the HPLC pump was manually stopped 22 min into the run, while the NMR spectrometer continued to acquire data. This allowed us to monitor the effects of active diffusion upon the NMR lineshapes. Figs. 9 and 10 show the response of the DSS

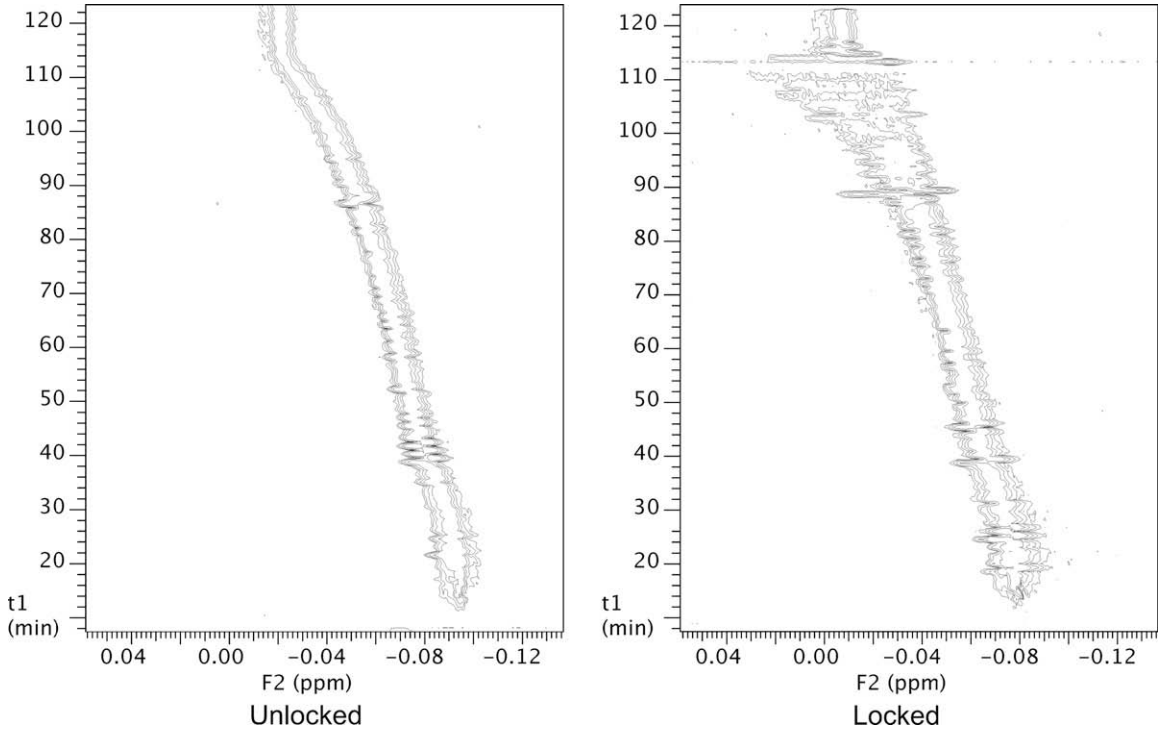

Fig. 6. Unlocked versus locked. A comparison of the linewidth of the DSS resonance in LC-NMR data acquired either without (left) or with (right) a ^2H lock on D_2O/HOD. The broadening of the DSS resonance caused by the tugging of the ^2H lock on D_2O/HOD is especially noticeable from 90 to 115 min, but some broadening is visible throughout the entire dataset. Both datasets were plotted with the same *F2* and "*t1*" expansions and the same vertical scales. (Both datasets were acquired with 16 transients per increment and a 1% ramp. Only the status of the lock was changed between datasets.)

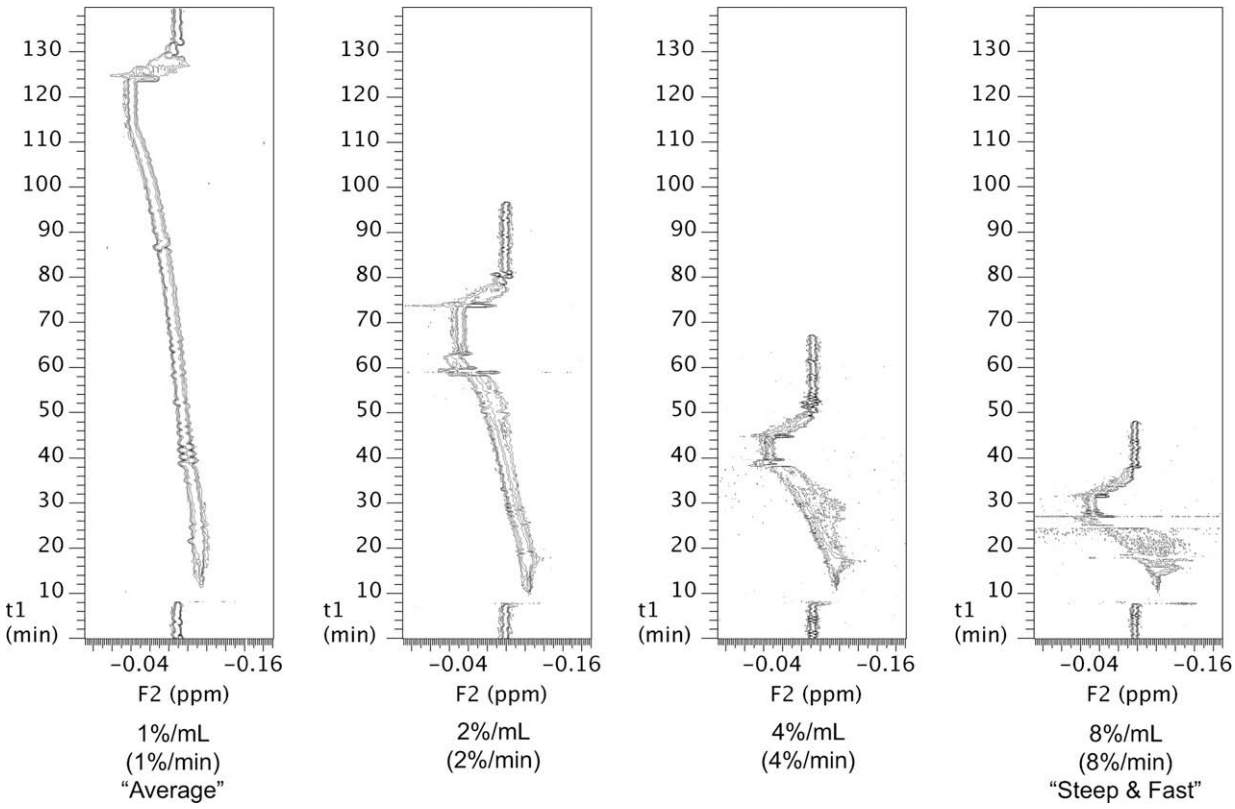

Fig. 7. Different ramp rates. A comparison of the linewidth of the DSS resonance in LC-NMR data acquired with 0–100% CH_3CN ramps that occurred over 100 min (1%/min), 50 min (2%/min), 25 min (4%/min), and 12.5 min (8%/min) (left-to-right). These data show how steeper and faster solvent-gradient ramps degrade lineshapes. All spectra were acquired at a flow rate of 1 mL/min. All datasets were plotted with the same *F2* expansion, but the different experimental conditions necessitated different "*t*1" expansions and vertical scales. All spectra were acquired identically other than the ramp rate and the number of transients per increment (which was adjusted to 16, 8, 4, and 2; left-to-right).

lineshape during this experiment. They show that the DSS lineshape recovers from a 20-Hz-wide lump the moment the pump was stopped (at 23 min into the run), to a 4.6-Hz-wide split singlet within 90 s of stopping the pump, to a 3.4-Hz-wide split singlet within 150 s, to a 2.1 Hz singlet within 300 s (5 min). The DSS linewidth was 0.86 Hz (±0.06 Hz) at the start of the experiment (in 50:50 CH_3CN:D_2O, where it was shimmed).

2.6. Shimming

The DSS lineshape in Fig. 9 did not recover back to the 0.86 Hz seen at the start of the dataset, which nicely illustrates an aspect of shimming that influences all LC–NMR* experiments that use a solvent gradient. The best lineshapes are always obtained when the same solvent composition is used to both shim the probe and acquire the data. As the solvent composition used for data acquisition changes further away from the solvent composition used for shimming, the lineshape will increasingly degrade. When the solvent composition is returned to that used for shimming, the lineshape will recover (due to the fixed geometry of both the flow cell and the solvent, and no meniscus). This indicates that a user should shim on a solvent composition that is in the mid-point of the solvent-gradient ramp (for on-flow solvent-gradient experiments). For that reason, the data acquired in this study were always acquired by only shimming when the probe was equilibrated with 50:50 CH_3CN:D_2O. In contrast to tube-based probes that must be reshimmed on every sample tube, it is the author's experience that once a flow probe is shimmed, it remains well shimmed for days – unless the solvent composition is changed. So although the DSS lineshape in Figs. 9 and 10 didn't recover *during the run* to the 0.86 Hz resolution obtained during the first increments, it did recover to that resolution as soon as the solvent composition was returned to 50:50 CH_3CN:D_2O (for the start of the next run).

Figs. 6–10 show that there is an upper limit to the steepness of the solvent gradients that can (or should) be used in LC–NMR*. This limit is influenced by flow rate (as shown), LC-column size, NMR-flowcell size, and the magnetic susceptibilities of the solvents being mixed (data not shown). A limit of 1%/mL and 1%/min was reasonable here, for a 4.6-mm LC column in a 60-μL NMR flow cell. There have been other reports that solvent gradients can cause NMR linebroadenings, but with less quantification of the limit or under different conditions [46,47]. Proposed workarounds to this problem have included stopped-flow LC–NMR*, SPE–NMR column trapping, and "waiting before NMR acquisition" [47–50]; a mobile-phase compensation method has also been proposed as a way to actually increase this limit [51].

2.7. Acquisition parameters

Lastly, we compared the effect of the balance between the number of transients and the number of increments during on-flow solvent-gradient LC–NMR* experiments. In a given amount of experiment time, you can either have more transients (to increase signal-to-noise for each increment) or more increments (to increase the "chromatographic resolution" of the NMR experiment). During an on-flow solvent-gradient experiment, as the number of transients (per increment) increases, the risk increases that a tugging lock will broaden the NMR linewidths (because there are fewer Scout-Scans for a given change in the solvent gradient). This effect is seen in Figs. 11 and 12, which show the ^1H resonance of

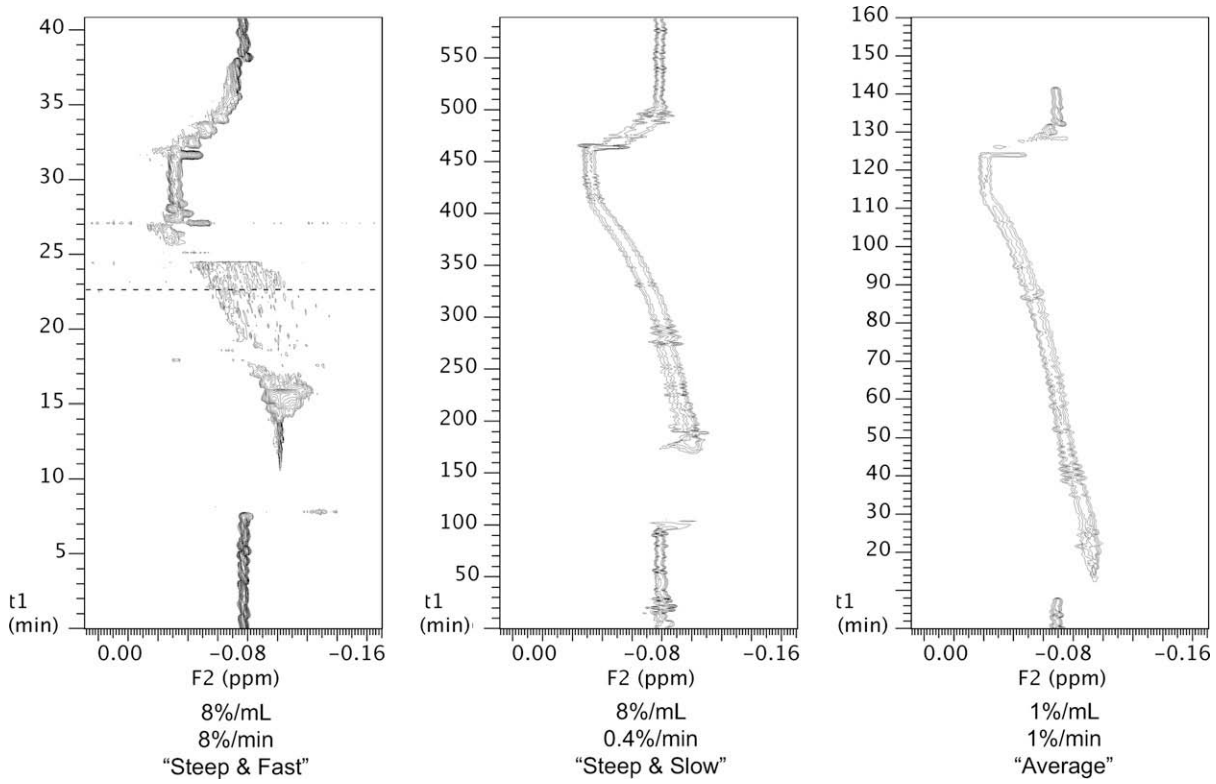

Fig. 8. Different ramp speeds. A comparison of the linewidth of the DSS resonance acquired with 0–100% CH_3CN ramps of different speeds. The 0–100% ramps that were used (left-to-right) occurred over 12.5 min (at 1.0 mL/min, so 8%/mL and 8%/min; "steep and fast"), 250 min (at 0.05 mL/min, so 8%/mL but 0.4%/min; "steep and slow"), and 100 min (at 1.0 mL/min, so 1%/mL and 1%/min; "average"). The middle "steep and slow" spectrum was comparable to the left-hand "steep and fast" spectrum except that the chromatography was run 20 times slower. The right-hand spectrum is displayed as a comparison spectrum that shows acceptably good lineshape. The total time of the middle experiment was almost 600 min, which accounted for the 1D control spectra acquired before and after the 0–100% ramp (data shown). All spectra were acquired in the same way other than the ramp rate, the flow rate, and the number of transients per increment (which was adjusted to 2, 40, and 16; left-to-right). All datasets were plotted with the same *F*2 expansion, but the different experimental conditions necessitated different time-axis expansions and different vertical scales. The spectrum on the left has an increased vertical scale as compared to the other two spectra, so as to see the broad signals. (The dotted line on the spectrum on the left is for comparison to Fig. 9.) The spectrum on the right stopped data collection at 140 min; the spectrum on the left continued data acquisition until 48 min (with data after 41 min not shown for clarity). As a comparison, the DSS linewidths in the spectra at the top of the middle and right-hand figures (acquired during 500–600 and 130–140 min, respectively) ranged from ~0.92 to ~1.45 Hz (±0.49 Hz). (In this figure only, all data in this figure were baseline corrected in *F*2 for clarity. No zerofilling, weighting functions, or solvent subtraction were used.)

the formate ion acquired with three different sets of NMR conditions. The data acquired with four scans per increment (on the left) has narrower linewidths but a lower signal-to-noise than the data acquired with 32 scans per increment (in the middle). (Some aspects are easier to see in the stacked-plot version of the data shown in Fig. 12.) A dataset acquired with 16 scans per increment is shown on the right for comparison (extracted from the same dataset as is shown in Figs. 4 and 6–8); it was acquired 36 h earlier than the two left-most datasets, which were acquired with a fresh batch of mobile phase. Subtle differences between batches of mobile phase (possibly pH or water content) may be why the formate-ion resonance moves slightly sooner (near 100 min) in the right-hand dataset than in the two left-most datasets. The increased duration of a 32-scan acquisition adds an apparent artificial lag time to the vertical axis of the middle dataset.

3. Discussion

3.1. Chemical-shift referencing

The original question of whether to use an organic resonance or the water resonance as a fixed-position chemical-shift reference during a solvent-gradient experiment is answered by a simple inspection of Figs. 4 and 5. The drastically more-constant chemical shifts seen in Fig. 4 make it clear that maintaining the transmitter on the CH_3CN resonance gives much better NMR data than keeping water constant (as was used in Fig. 5), despite the fact that the latter method has been routinely reported in the literature [52–55]. The latter method is easy to run – either by locking on the D_2O/HOD ^2H resonance or by actively tracking the HOD/H_2O ^1H resonance – but it clearly produces misleading ^1H chemical-shift scales.

If an organic resonance should be used as a fixed-position chemical-shift reference, the next question is "which organic resonance should be used?" Although conventional solution-state NMR has defined that a dilute solution of TMS in $CDCl_3$, with the ^1H resonance of the TMS set to 0.0 ppm, is the primary chemical-shift reference standard, most LC–NMR* experiments use reversed-phase (aqueous) HPLC conditions, which precludes the use of TMS. DSS and TSP come to mind, but they are not usually added to most NMR samples, and more importantly their chemical shifts are known to be dependant upon solvent composition and pH (as discussed above). The most common HPLC (and LC–NMR*) mobile phase is acetonitrile:water, so we wanted to know how stable the ^1H chemical shift of CH_3CN was over the entire range of possible solvent compositions. We evaluated this here by comparing the ^1H chemical shift of CH_3CN to the ^1H chemical shifts of a number of other (potential) secondary standards during the solvent-gradient experiment.

Fig. 13 shows an expansion of the data shown in Fig. 4, re-plotted with a compressed time axis so as to emphasize ^1H chemical-shift movements. This figure shows the chemical-shift movements over the entire 0–100% CH_3CN ramp, for data acquired by keeping the

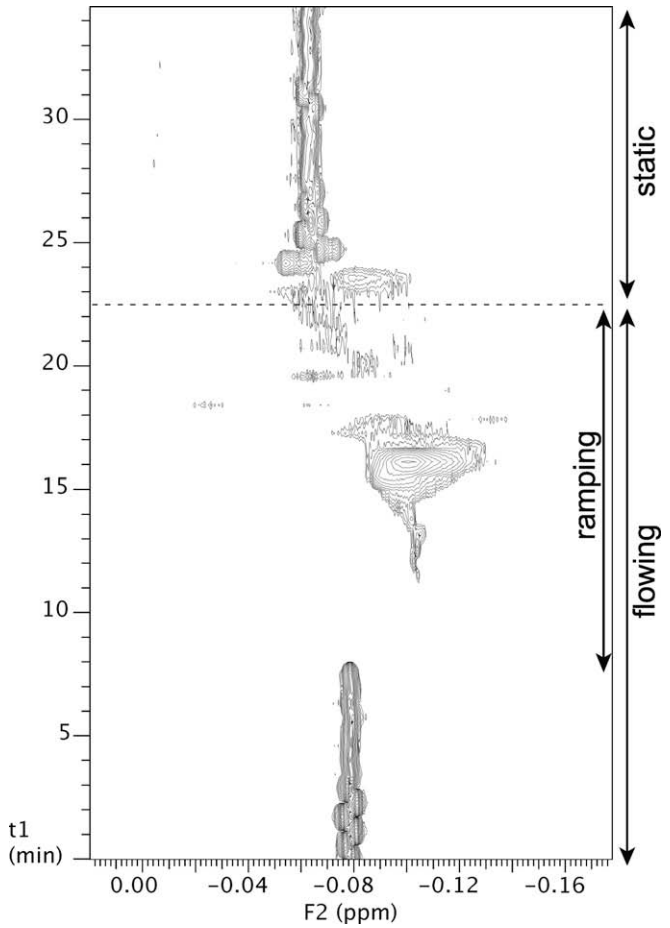

Fig. 9. The effects of static diffusion: contour plot. These data show the linewidth of the DSS resonance during an "8%/min 8%/mL" experiment where the pump was stopped 22 min into the run (at the dotted line) but NMR acquisition continued – so as to monitor the effects of diffusion. The spectra at the beginning of the run (from 0 to ca. 8 min along the time axis) were acquired on flowing and equilibrated 50:50 $CH_3CN:D_2O$, whereas the data acquired after 22 min were acquired on a solvent mixture that was no longer flowing, and was not equilibrated anywhere in the LC-NMR system other than by active diffusion happening within the NMR flow cell. The effect of stopping the pump can be seen by comparing the first 22 min of this spectrum to the first 22 min of the left-most spectrum in Fig. 8 (to the dotted line), which was run with the same conditions except for the stopping of the pump. (Acquired with eight transients per increment.)

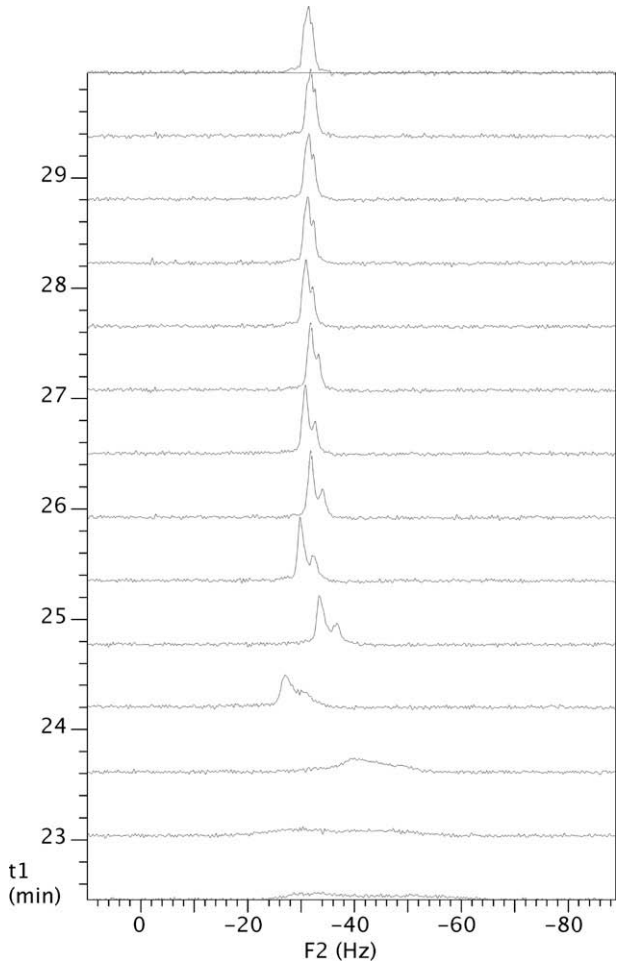

Fig. 10. The effects of static diffusion: stacked plot. An expansion of the data shown in Fig. 9, now displayed as a stacked plot to more easily monitor the linewidths of the DSS resonance. The HPLC pump was manually stopped during the first displayed spectrum. All the remaining increments were acquired while the mobile phase was static.

^1H resonance of the CH_3CN fixed at 1.95 ppm. The question here is "which NMR resonance has the most stable chemical shift?" Clearly water is bad, but which signal is good enough?

First of all, it appears as if no resonance is perfectly well behaved. The DSS singlet tracks with the CH_2Cl_2 resonance, and maybe the last half of the CH_3OH resonance. The DSS methylene at 0.5 ppm tracks fairly well with the CH_3OH and anomeric sucrose signals. The CH_3OH signal somewhat tracks the sucrose anomeric signal, which tracks a few of the other sucrose resonances, but many of the other sucrose resonances track in the other direction. The $CHCl_3$ signal (when visible) tracks fairly well with the CH_3CN signal except at the very end. The formate signal tracks somewhat with the CH_3CN signal until about 85% CH_3CN when the formate signal then moves drastically. The $CHCl_3$ and formate signals track in one direction compared to CH_3CN (as do the DSS downfield methylene and most of the sucrose signals), whereas the DSS singlet, DSS 0.5 ppm, CH_3OH, CH_2Cl_2, and sucrose anomeric signals track in the other direction. Overall, however, most of the signals drift well under 0.2 ppm (in contrast to the 2.4 ppm changes seen in Fig. 5), which further supports that keeping the CH_3CN signal at a fixed frequency is the correct way to acquire the data.

The movement of the CH_3CN resonance (relative to all the organic [non-water] signals) is close to the mathematical average of all of these other relative chemical-shift movements. We were limited to evaluating compounds that were not significantly retained by the HPLC column and were soluble and visible over the entire 0–100% CH_3CN solvent-gradient ramp, but based upon these data, it appears that the ^1H resonance of CH_3CN is indeed well behaved, and can serve as a suitable secondary chemical-shift standard. (Likewise, a recent ^{29}Si LC–NMR study also concluded that, when all the chemical shifts in the sample move as a function of solvent composition, then it is important to select a reference compound whose chemical shift moves most like the solutes of interest [27].)

Once it was shown how important it was to maintain the CH_3CN resonance at a fixed frequency, the Scout-Scan technique proves itself to be an appropriate way to do so. This is because it works despite the tugging caused by the ^2H lock signal on D_2O/HOD (which is always trying to keep the ^1H resonance of HOD/H_2O at a fixed frequency; a process that Fig. 5 shows is inappropriate).

3.2. Other variables

Fig. 6 shows that the ^2H lock can actually degrade lineshapes when solvent gradients are happening during the NMR acquisition (as can happen during on-flow LC–NMR* experiments). The choice

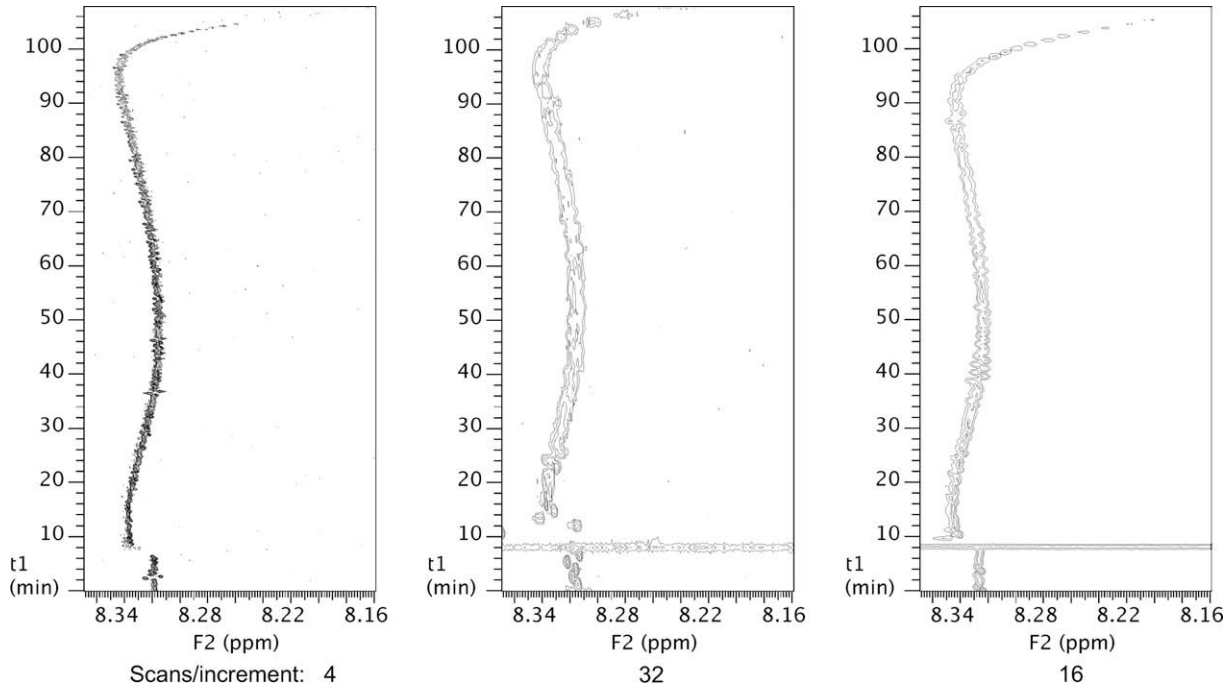

Fig. 11. Sampling rate. This is a comparison of the linewidth of the formate resonance acquired by using 4 (left), 32 (middle), or 16 (right) scans per increment. All other LC-NMR parameters and conditions used to acquire the three datasets were identical. (Acquired with a 0–100% ramp at 1.0 mL/min over 100 min.)

of whether or not to use a ^{2}H lock on water (D_2O) is different for on-flow versus stopped-flow LC–NMR* experiments. The ^{2}H lock on D_2O/HOD can be an asset during stopped-flow experiments, as long as the chemical-shift scale and possibly the transmitter are set appropriately, because the ^{2}H lock can compensate for magnet drift. It can also be an asset for isocratic (constant-solvent) on-flow experiments. But for on-flow solvent-gradient runs, the ^{2}H lock on D_2O/HOD must be used very carefully, or, better yet, turned off. The steeper the solvent gradient, the more important it is to turn off the ^{2}H lock.

To allow good lineshapes to be maintained during on-flow LC–NMR runs, the data show that the solvent-gradient ramps should typically be limited to less than 1%/min (at a flow rate of 1.0 mL/min; in the NMR flow-cell volume used here; with the solvent mixtures used here). Faster solvent ramps will result in degraded lineshapes that cannot be shimmed out, and which will reduce overall signal-to-noise. If a steep solvent ramp (by volume) must be used, these data show that slowing down the flow rate will help reduce the degradation of the lineshape. (The author has found that this sometimes does not work, especially when concentrated solutes

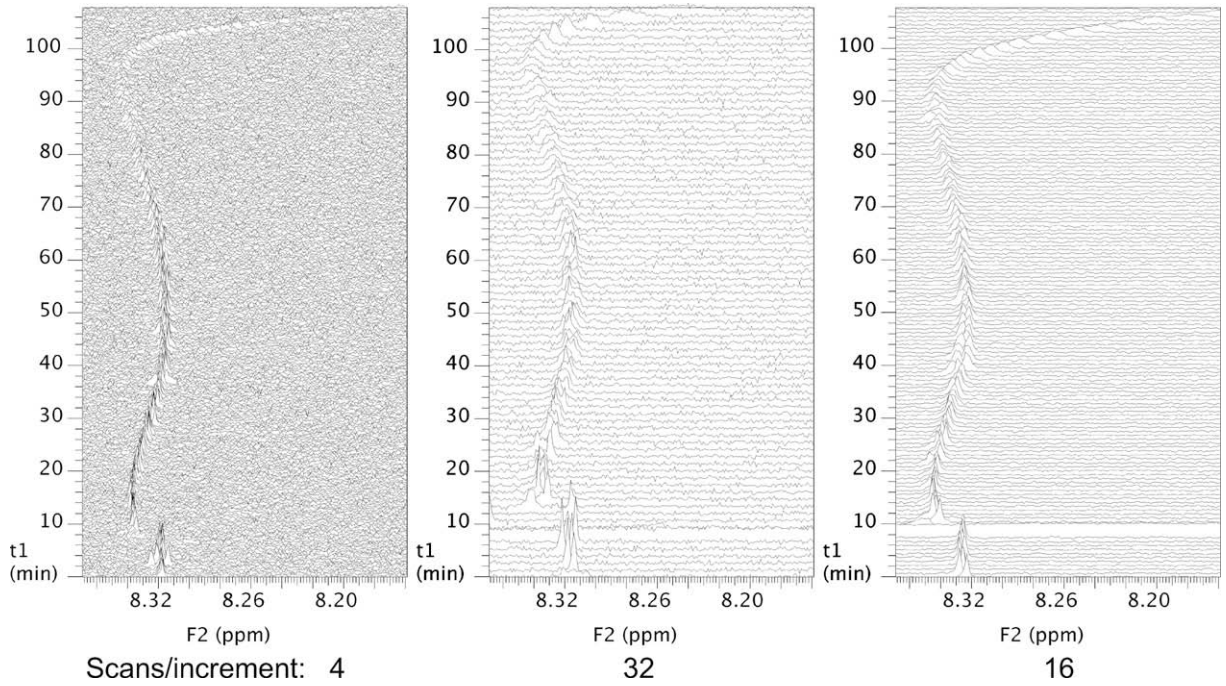

Fig. 12. Sampling rate. A stacked-plot version of Fig. 11 to facilitate comparisons of the linewidths and signal-to-noise.

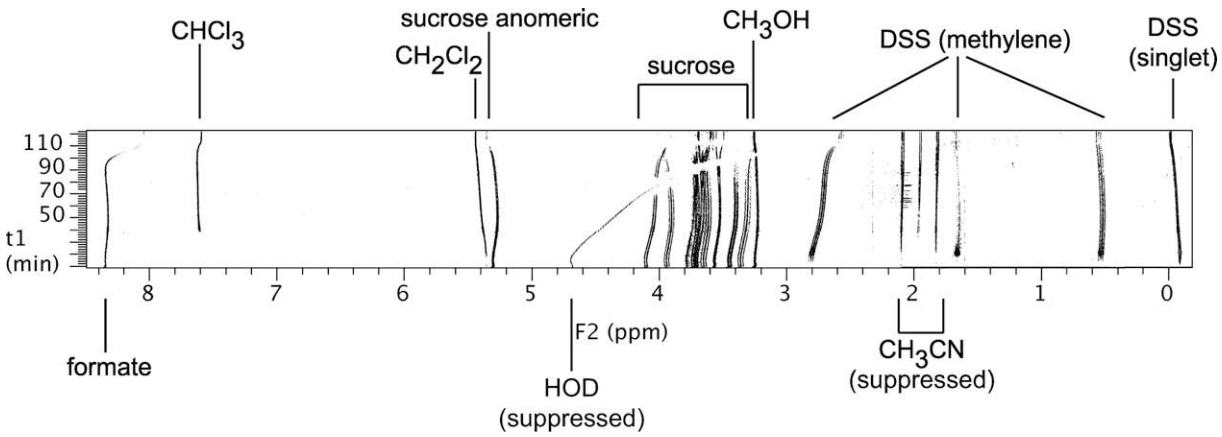

Fig. 13. Relative chemical-shift movements. This is the same data as is shown in Fig. 4 but labeled and expanded (and compressed along "*t*1") for clarity.

elute, and that diffusion does not always happen in the NMR flow cell, presumably due to stable density gradients.) The author has also seen that this 1%/min limit is influenced by the choice of solvents used in the mobile phase; the rate limit is probably directly determined by the difference in magnetic susceptibilities between the two solvents (data not shown).

It is important to recognize that different shimming methods can have different effects in LC–NMR∗. When the mobile phase is a combination of CH_3CN and D_2O, then shimming on the ^2H signal – using either the lock signal or a ^2H pulsed-field-gradient (PFG) map – will shim on the water (HOD/D_2O) signal, which is notoriously sensitive to broadening from both temperature gradients and solvent-composition gradients (as discussed above). If either temperature- or solvent-gradients exist, and if the ^2H signal is used in any way for shimming, then when the uniquely broadened water resonance is made narrower using any of the shim gradients (for example, temperature gradients are often linearly axially dependant, like the z1 shim, so the temperature-gradient-induced linebroadening can then be offset by missetting z1) then the "removed resultant linebroadening" that was only on the HOD/H_2O resonance gets (erroneously) transferred to every other resonance in the ^1H spectrum. If you do this, you just convert a ^1H spectrum with narrow organic resonances and a broad water resonance into an (undesirable) spectrum with broad organic resonances and a narrow water resonance. Similar effects can sometimes be seen when the water resonance is broadened by a concentration gradient; this presumably happens because the concentration gradient has a linear component caused by the solvent flowing unidirectionally into the NMR flow cell.

In contrast, when ^1H PFG shimming is used on $CH_3CN:D_2O$, the ^1H signal is dominated by the ^1H resonance of CH_3CN, which is a more well-behaved resonance, and this results in the narrowest possible ^1H linewidths for all of the organic resonances (but it may leave the HOD/H_2O signal broad, which is proper). This is also true in ^1H spectral shimming, (depending upon which ^1H resonance is used), and is true to a lesser extent in ^1H free-induction-decay (FID) shimming, depending upon how much of the FID is made up of the HOD/H_2O signal.

In on-flow LC–NMR∗ experiments, the user must strike a balance between how many transients per spectrum to use versus how many spectra (increments) can be obtained. Unlike with conventional 2D NMR spectra, which typically have no specific limit to the duration of the experiment, on-flow LC–NMR∗ experiments have a fixed duration, which is limited by the longest retention time (of the most-retained chromatographic peak). The pseudo-2D nature of LC–NMR∗ experiments means that there is a maximum number of "transients × increments" that can be obtained during this time. (The repetition rate of an on-flow NMR experiment does not have the same dependence upon T_1 as in a conventional 2D spectra because the flowing mobile phase can effectively shorten T_1 [56].) In addition, each solute has only a finite residence time in the NMR flow cell (which depends upon the flow rate of the mobile phase and the bandwidth of the chromatographic peak), which sets an upper limit on the NMR signal-to-noise that can be obtained (at a given flow rate). Within these boundaries, if the number of transients per increment is large (giving fewer increments), you will get the maximum possible NMR signal-to-noise, but you will lose chromatographic resolution. If a solvent gradient is being used, you will also be maximally susceptible to NMR linebroadenings caused by chemical-shift movements arising from solvent changes during the signal averaging of that increment. (The NMR linebroadenings arise from an inhomogeneous magnetic susceptibility in the flow cell, and are caused by uneven mixing of the solvents.) Conversely, if the number of transients per increment is small (giving more increments), you will get a lower NMR signal-to-noise, but the chromatographic resolution will be maximized and the NMR linebroadenings caused by solvent gradients will be reduced. This effect can be seen in Figs. 11 and 12, which show the effects of using three different combinations of "number of transients" versus "number of increments" in an on-flow solvent-gradient LC–NMR experiment. (The formate resonance is shown in these figures because it is a well-separated singlet that undergoes one of the bigger chemical-shift changes during the solvent-gradient ramp, although similar effects can be seen on virtually all resonances in the spectra.) As the chemical shift of a resonance moves faster because of the solvent-composition ramp, the number of transients per increment should be made smaller, so as to allow narrow linewidths to be observed. The 4-scan-per-increment data (on the left in Figs. 11 and 12) produces narrower NMR linewidths than the 16-scan-per increment data (on the right in Figs. 11 and 12), and they both produce narrower linewidths than the 32-scan-per-increment data (in the middle). In contrast, the 32-scan data has better signal-to-noise than the 4-scan data. (The vertical scales of the three spectra in these two figures were not scaled to compensate for the differing number of scans per increment.) These effects can be seen throughout the entire datasets, but are especially evident in the region between 10 and 50 min. The data illustrate the importance of selecting a good balance between the number of transients and the number of increments in LC–NMR∗; a balance that depends upon the solvent-gradient rate, the magnitude of chemical-shift changes (as a function of solvent composition), and the desired narrowness of linewidths. Note that this balance is less critical if the NMR resonances are naturally broad or if solvent gradients are not used (i.e., if an isocratic LC method

is used), and it is a non-issue if the NMR data is not acquired on-flow (i.e., if it is a stopped-flow LC–NMR* experiment).

3.3. Sources of error

Lastly, we can now summarize the sources of error for measuring chemical shifts in on-flow solvent-gradient LC–NMR*. First, it has been shown here that water moves enormously during a 0–100% gradient, so it shouldn't ever be used as a reference signal (Fig. 1). Second, it has been demonstrated here how this moving D_2O resonance drags the ^2H lock during signal averaging whenever D_2O is used as a lock signal (Fig. 6), which then moves and broadens the observed resonances. Third, the literature (discussed above) contains many examples of solute resonances moving – sometimes in different directions – during a solvent gradient, and that effect has also been seen here (Fig. 13). (This complicates both the reporting of the chemical shifts, and the ability of others in repeating the work, because the solvent composition in the NMR flow cell may not be accurately known when the chemical shifts are measured.) Fourth, because a solvent gradient changes the proportion of solvents in the mobile phase, which can generate different amounts of radiation-damping-induced NMR linebroadenings in the solvent resonances (as a function of concentration), this can create a variable uncertainty in the Scout-Scan determination of the solvent-resonance frequency. This has not been observed to be a problem, but note that the small tip angles used in the Scout-Scan method will not avoid the radiation-damping effect. (The radiation-damping-induced NMR linebroadenings are a bigger problem in cryogenic probes and higher field magnets, where the *Q* of the probe and the signal response is highest.) Fifth, concentration-dependent frequency shifts of the solvent resonances due to flux density changes are readily observable on solvent signals [57–59], which can add additional movements in – and hence uncertainties to – the measurement of the solvent signal's frequency. (These shifts are the reason post-processing DSP [digital signal processing] notch filters need to be progressively moved "off-resonance" as solvent concentration increases.) Lastly, the author has also observed that a mis-set lock phase can induce phase distortions in solute resonances whenever PFG-solvent-suppression sequences like WET [41] are used (data not shown). This effect is a sensitive test for how accurately the lock phase has been adjusted, and could also contribute to chemical-shift measurement errors.

4. Conclusions

These data show that using the water resonance in any way to reference, shim, or lock the NMR spectra in LC–NMR* experiments is unsatisfactory, specifically for on-flow solvent-gradient experiments, despite the regularity with which such data appear in the literature [52–55]. This is true regardless of whether the water resonance is used as a ^2H lock (for D_2O) or as an internal standard (for H_2O or HOD). Using the ^1H resonance of CH_3CN as a secondary reference and a signal for shimming (and effectively as a lock signal) is shown here to have many advantages and be a much better choice. Software tools for referencing on the CH_3CN resonance exist, are automated and easy to use, and work under all solvent conditions. When comparing CH_3CN as a secondary chemical-shift reference to other available compounds, it appears to be both a good option and the best option available.

These conclusions are applicable to any experiments that use LC–NMR, or incorporate either it or related techniques (such as LC–NMR–MS, LC–PDA–NMR–MS, LC–MS–NMR–CD, CapLC–NMR, LC–SPE–NMR, etc. [4]; hence our use here of the term LC–NMR*). They certainly apply to LC–NMR* experiments that use solvent gradients and are acquired "on-flow". Some of these conclusions also apply to isocratic on-flow experiments, and some apply to solvent-gradient stopped-flow experiments. These conclusions should also apply to other flow NMR methods such as flow-injection-analysis NMR (FIA-NMR) [60] and direct-injection NMR (DI-NMR) techniques [43] such as VAST or BEST. They may also apply to conventional (i.e., 5 mm) tube-based experiments when the samples either have temperature gradients or use solvent mixtures that may not be sufficiently well mixed.

5. Experimental

All NMR spectra were acquired on a Varian INOVA 500-MHz NMR spectrometer running VNMR software. It was equipped with an H{C, N} IFC flow probe with an active volume of 60 μL (115 μL total volume) maintained at ~293 K (20 °C). All NMR data were acquired with the following conditions unless otherwise indicated: 2.048 s acquisition time (at), 0.001 s recovery delay (d1), 8000 Hz spectral width, 32,768 complex points (np), 2 steady-state scans, 16 scans (nt), no digital signal processing, no ^2H lock, two-frequency solvent suppression with the transmitter on CH_3CN, and 21.5-ms seduce pulses for WET. Unless otherwise indicated, all NMR data were processed without zerofilling, weighting functions, solvent-subtraction notch filters (ssfilter), or baseline correction, so as to best evaluate the raw data.

The chromatography was performed with a Varian 9012 pump, a 9050 UV detector, an LC-NMR Analyte Collector, and a Varian ResElut 5-micron C18 HPLC column (150 × 4.6 mm, #1215-9012). The default HPLC method was [(time) action]: (0.0) 50:50 $CH_3CN:D_2O$; (5.00) 50:50 $CH_3CN:D_2O$; (5.01) 0:100 $CH_3CN:D_2O$; (10.0) 0:100 $CH_3CN:D_2O$; (110.0) 100:0 $CH_3CN:D_2O$; (120.0) 100:0 $CH_3CN:D_2O$; (125.0) 50:50 $CH_3CN:D_2O$; (130.0) End, as is graphically shown in Fig. 2. Experiments were then run using different flow rates (the default was 1.0 mL/min) and different ramp durations/rates (the default was 1%/min = 1%/mL).

The solvents used were acetonitrile (CH_3CN; EM Science Omnisolv Glass Distilled; #AX0142-1) and D_2O (99.9 at.%D, Isotec #151882). No significant measures were used to keep the (hygroscopic) D_2O free of absorbed water during use, so it contained a measurable amount of HOD. Both solvents were spiked with a cocktail of compounds that were dissolved in 50:50 $CH_3CN:D_2O$, so they each contained (listed in chemical-shift order; amounts added and final concentrations listed in brackets): DSS (sodium 2,2-dimethyl-2-silapentane-5-sulfonate hydrate) [34.7 mg/L, 0.147 mM]; sucrose [101.9 mg/L, 0.298 mM]; CH_3OH [25 μL/L, 0.62 mM]; CH_2Cl_2 [37.5 μL/L, 0.63 mM]; $CHCl_3$ [75 μL/L, 0.91 mM]; and sodium formate [41.8 mg/L, 0.615 mM]. As the spiking cocktail was dissolved in 50:50 $CH_3CN:D_2O$, each solvent also contained CH_3CN [5 mL/L, ~95 mM] and D_2O [5 mL/L, ~275 mM].

Acknowledgments

I would like to thank Steve Smallcombe, Karen Salomon, and Varian Associates for their help in making these studies possible, and to Gus Wang for useful discussions.

References

[1] R.K. Harris, E.D. Becker, S.M. Cabral De Menezes, R. Goodfellow, P. Granger, NMR nomenclature. Nuclear spin properties and conventions for chemical shifts (IUPAC recommendations 2001), Pure Appl. Chem. 73 (2001) 1795–1818.
[2] G.V.D. Tiers, Proton nuclear resonance spectroscopy. 1. Reliable shielding values by 'internal referencing' with tetramethylsilane, J. Phys. Chem. 62 (1958) 1151–1152.
[3] C.R. Morcombe, K.W. Zilm, Chemical shift referencing in MAS solid state NMR, J. Magn. Reson. 162 (2003) 479–486.

[4] P.A. Keifer, Flow techniques in NMR spectroscopy, Annu. Rep. NMR Spectrosc. 62 (2007) 1–47.
[5] E. Lenz, S. Taylor, C. Collins, I.D. Wilson, D. Louden, A. Handley, Flow injection analysis with multiple on-line spectroscopic analysis (UV, IR, ^{1}H NMR and MS), J. Pharm. Biomed. Anal. 27 (2002) 191–200.
[6] J.L. Markley, A. Bax, Y. Arata, C.W. Hilbers, R. Kaptein, B.D. Sykes, P.E. Wright, K. Wuthrich, Recommendations for the presentation of NMR structures of proteins and nucleic acids, Pure Appl. Chem. 70 (1998) 117–142.
[7] G.V.D. Tiers, R.I. Coon, Preparation of sodium 2,2-dimethyl-2-silapentane-5-sulfonate, a useful internal reference for N.S.R. spectroscopy in aqueous and ionic solutions, J. Org. Chem. 26 (1961) 2097–2098.
[8] D.S. Wishart, C.G. Bigam, J. Yao, F. Abildgaard, H.J. Dyson, E. Oldfield, J.L. Markley, B.D. Sykes, 1H, 13C and 15N chemical shift referencing in biomolecular NMR, J. Biomol. NMR 6 (1995) 135–140.
[9] D.H. Live, S.I. Chan, Use of DSS as an internal standard in PMR studies of nucleic acid interactions, Org. Magn. Reson. 5 (1973) 275–276.
[10] L. Pohl, M. Eckle, Sodium 3-trimethylsilyltetradeuteriopropionate, a new water-soluble standard for ^{1}H NMR, Angew. Chem. Int. Ed. Engl. 8 (1969) 381.
[11] W. McFarlane, R.F.M. White, Techniques of High Resolution Nuclear Magnetic Resonance Spectroscopy, CRC Press, Cleveland OH, 1972.
[12] S. Hayashi, M. Yanagisawa, K. Hayamizu, Nuclear magnetic resonance chemical shifts of pure organic solvents determined by magic angle spinning, Anal. Sci. 7 (1991) 955–957.
[13] G. Dyke Tiers, Detection of oriented association via NMR dilution shifts in tetramethylsilane solvent. 4. Temperature coefficients for perfluoroalkyl halide systems, J. Fluorine Chem. 102 (2000) 175–184.
[14] D.G. De Kowalewski, C. los Santos, E. Marceca, Use of an internal reference in carbon-13 chemical shift measurements, Magn. Reson. Chem. 28 (1990) 1–4.
[15] R.E. Hoffman, Variations on the chemical shift of TMS, J. Magn. Reson. 163 (2003) 325–331.
[16] R.E. Hoffman, E.D. Becker, Temperature dependence of the 1H chemical shift of tetramethylsilane in chloroform, methanol, and dimethylsulfoxide, J. Magn. Reson. 176 (2005) 87–98.
[17] R.E. Hoffman, Measurement of magnetic susceptibility and calculation of shape factor of NMR samples, J. Magn. Reson. 178 (2006) 237–247.
[18] D.H. Live, S.I. Chan, Bulk susceptibility corrections in nuclear magnetic resonance experiments using superconducting solenoids, Anal. Chem. 42 (1970) 791–792.
[19] M.R. Bacon, G.E. Maciel, Solvent effects on the five shielding constants in tetramethylsilane and cyclohexane, J. Am. Chem. Soc. 95 (1973) 2413–2426.
[20] P. Granger, M. Bourdonneau, O. Assemat, M. Piotto, NMR chemical shift measurements revisited: high precision measurements, Concepts Magn. Reson. 30A (2007) 184–193.
[21] A. DeMarco, pH dependence of internal references, J. Magn. Reson. 26 (1977) 527–528.
[22] D.S. Wishart, B.D. Sykes, Chemical shifts as a tool for structure determination 239 (1994) 363–392.
[23] R.E. Hoffman, D.B. Davies, Temperature dependence of NMR secondary references for water-d2 and dimethyl-d6 sulfoxide solutions, Magn. Reson. Chem. 26 (1988) 523–525.
[24] Y.F. Lam, G. Kotowycz, Caution concerning the use of sodium 2,2-dimethyl-2-silapentane-5-sulfonate (DSS) as a reference for proton NMR chemical shift studies, FEBS Lett. 78 (1977) 181–183.
[25] A. Shimizu, M. Ikeguchi, S. Sugai, Appropriateness of DSS and TSP as internal references for 1H NMR studies of molten globule proteins in aqueous media, J. Biomol. NMR 4 (1994) 859–862.
[26] N. Funasaki, M. Nomura, S. Ishikawa, S. Neya, NMR chemical shift references for binding constant determination in aqueous solutions, J. Phys. Chem. B 105 (2001) 7361–7365.
[27] V. Blechta, M. Kurfurst, J. Sykora, J. Schraml, High-performance liquid chromatography with nuclear magnetic resonance detection applied to organosilicon polymers. Part 2. Comparison with other methods, J. Chromatogr. A 1145 (2007) 175–182.
[28] M. Kriat, S. Confort-Gouny, J. Vion-Dury, M. Sciaky, P. Viout, P.J. Cozzone, Quantitation of metabolites in human blood serum by proton magnetic resonance spectroscopy. A comparative study of the use of formate and TSP as concentration standards, NMR Biomed. 5 (1992) 179–184.
[29] J.S. Nowick, O. Khakshoor, M. Hashemzadeh, J.O. Brower, DSA: a new internal standard for NMR studies in aqueous solution, Org. Lett. 5 (2003) 3511–3513.
[30] D.D. Laws, D.S. Wishart, R.H. Havlin, M. Westmeyer, B.D. Sykes, E. Oldfield, N,N',N''-trimethyl(2-trimethylsilyl)ethylammonium iodide – a universal internal standard for H-1, C-13, and N-15 NMR, J. Magn. Reson. Ser. B 108 (1995) 274–275.
[31] V. Pinciroli, R. Biancardi, N. Colombo, M. Colombo, V. Rizzo, Characterization of small combinatorial chemistry libraries by 1H NMR. Quantitation with a convenient and novel internal standard, J. Comb. Chem. 3 (2001) 434–440.
[32] S.W. Gerritz, A.M. Sefler, 2,5-dimethylfuran (DMFu): an internal standard for the "Traceless" quantitation of unknown samples via 1H NMR, J. Comb. Chem. 2 (2000) 39–41.
[33] J. Schraml, Hexamethyldisilane – a convenient solvent and secondary proton-NMR reference, Collect. Czech. Chem. Commun. 41 (1976) 231–233.
[34] K.L. Rinehart, W.A. Nilsson, H.A. Whaley, Sterculic acid: nuclear magnetic resonance spectrum and structure, J. Am. Chem. Soc. 80 (1958) 503–504.
[35] E.J. Corey, G. Slomp, S. Dev, S. Tobinaga, E.R. Glazier, Detection and structural analysis of furans by proton magnetic resonance, J. Am. Chem. Soc. 80 (1958) 1204–1206.
[36] H.E. Gottlieb, V. Kotlyar, A. Nudelman, NMR chemical shifts of common laboratory solvents as trace impurities, J. Org. Chem. 62 (1997) 7512–7515.
[37] J.T. Arnold, M.E. Packard, Variations in absolute chemical shift of nuclear induction signals of hydroxyl groups of methyl and ethyl alcohol, J. Chem. Phys. 19 (1951) 1608–1609.
[38] W.G. Schneider, H.J. Bernstein, J.A. Pople, Proton magnetic resonance chemical shift of free (gaseous) and associated (liquid) hydride molecules, J. Chem. Phys. 28 (1958) 601–607.
[39] A.J. Hartel, P.P. Lankhorst, C. Altona, Nucleic acid constituents. 24. Thermodynamics of stacking and of self-association of the dinucleoside monophosphate m26A-U from proton NMR chemical shifts: differential concentration temperature profile method, Eur. J. Biochem. 129 (1982) 343–357.
[40] L.P.M. Orbons, G.A. Van der Marel, J.H. Van Boom, C. Altona, An NMR study of polymorphous behavior of the mismatched DNA octamer d(m5C-G-m5C-G-A-G-m5C-G) in solution. The B-duplex and hairpin forms, Eur. J. Biochem. 170 (1987) 225–239.
[41] S.H. Smallcombe, S.L. Patt, P.A. Keifer, WET solvent suppression and its applications to LC NMR and high-resolution NMR spectroscopy, J. Magn. Reson. A 117 (1995) 295–303.
[42] S.L. Patt, Single- and multiple-frequency-shifted laminar pulses, J. Magn. Reson. 96 (1992) 94–102.
[43] P.A. Keifer, S.H. Smallcombe, E.H. Williams, K.E. Salomon, G. Mendez, J.L. Belletire, C.D. Moore, Direct-injection NMR (DI-NMR): a flow NMR technique for the analysis of combinatorial chemistry libraries, J. Comb. Chem. 2 (2000) 151–171.
[44] E. Kupce, R. Freeman, Techniques for multisite excitation, J. Magn. Reson. A 105 (1993) 234–238.
[45] E. Kupce, R. Freeman, "Template excitation" in high-resolution NMR, J. Magn. Reson. A 106 (1994) 135–139.
[46] D.A. Laude Jr., C.L. Wilkins, Reverse-phase high-performance liquid chromatography/nuclear magnetic resonance spectrometry in protonated solvents, Anal. Chem. 59 (1987) 546–551.
[47] M.E. Lacey, Z.J. Tan, A.G. Webb, J.V. Sweedler, Union of capillary high-performance liquid chromatography and microcoil nuclear magnetic resonance spectroscopy applied to the separation and identification of terpenoids, J. Chromatogr. A 922 (2001) 139–149.
[48] L. Griffiths, R. Horton, Optimization of LC-NMR. III. Increased signal-to-noise ratio through column trapping, Magn. Reson. Chem. 36 (1998) 104–109.
[49] J.A. de Koning, A.C. Hogenboom, T. Lacker, S. Strohschein, K. Albert, U.A.T. Brinkman, Online trace enrichment in hyphenated liquid chromatography–nuclear magnetic resonance spectroscopy, J. Chromatogr. A 813 (1998) 55–61.
[50] J.C. Lindon, J.K. Nicholson, I.D. Wilson, Directly coupled HPLC–NMR and HPLC–NMR–MS in pharmaceutical research and development, J. Chromatogr. B Biomed. Sci. Appl. 748 (2000) 233–258.
[51] D.A. Jayawickrama, A.M. Wolters, J.V. Sweedler, Mobile phase compensation to improve NMR spectral properties during solvent gradients, Analyst 128 (2003) 421–426.
[52] O. Cloarec, A. Campbell, L. Tseng, U. Braumann, M. Spraul, G. Scarfe, R. Weaver, J.K. Nicholson, Virtual chromatographic resolution enhancement in cryoflow LC-NMR experiments via statistical total correlation spectroscopy, Anal. Chem. 79 (2007) 3304–3311.
[53] M. Spraul, A.S. Freund, R.E. Nast, R.S. Withers, W.E. Maas, O. Corcoran, Advancing NMR sensitivity for LC-NMR–MS using a cryoflow probe: application to the analysis of acetaminophen metabolites in urine, Anal. Chem. 75 (2003) 1536–1541.
[54] J.C. Lindon, R.D. Farrant, P.N. Sanderson, P.M. Doyle, S.L. Gough, M. Spraul, M. Hofmann, J.K. Nicholson, Separation and characterization of components of peptide libraries using on-flow coupled HPLC–NMR spectroscopy, Magn. Reson. Chem. 33 (1995) 857–863.
[55] Available from: <http://www.hyphenation.de/index.php?area=background>.
[56] A.L. Bloom, J.N. Shoolery, High resolution of nuclear resonance signals in flowing samples, Phys. Rev. 90 (1953) 358.
[57] H.T. Edzes, The nuclear magnetization as the origin of transient changes in the magnetic field in pulsed NMR experiments, J. Magn. Reson. 86 (1990) 293–303.
[58] M.H. Levitt, Demagnetization field effects in two-dimensional solution NMR, Concepts Magn. Reson. 8 (1996) 77–103.
[59] S.Y. Huang, C. Anklin, J.D. Walls, Y.Y. Lin, Sizable concentration-dependent frequency shifts in solution NMR using sensitive probes, J. Am. Chem. Soc. 126 (2004) 15936–15937.
[60] P.A. Keifer, Flow injection analysis NMR (FIA-NMR) – a novel flow NMR technique that complements LC-NMR and direct injection NMR (DI-NMR), Magn. Reson. Chem. 41 (2003) 509–516.